Please cite this article in press as: Marqués-Torrejón et al., Cyclin-Dependent Kinase Inhibitor p21 Controls Adult Neural Stem Cell Expansion by Regulating Sox2 Gene Expression, Cell Stem Cell (2013), http://dx.doi.org/10.1016/j.stem.2012.12.001

Cell Stem Cell
Article

# Cyclin-Dependent Kinase Inhibitor p21 Controls Adult Neural Stem Cell Expansion by Regulating Sox2 Gene Expression

M. Ángeles Marqués-Torrejón,[1,2] Eva Porlan,[1,2,6] Ana Banito,[3,6] Esther Gómez-Ibarlucea,[4] Andrés J. Lopez-Contreras,[5] Óscar Fernández-Capetillo,[5] Anxo Vidal,[4] Jesús Gil,[3] Josema Torres,[1,*] and Isabel Fariñas[1,2,*]
[1]Departamento de Biología Celular
[2]Centro de Investigación Biomédica en Red sobre Enfermedades Neurodegenerativas
Universidad de Valencia, Valencia, 46100 Spain
[3]Cell Proliferation Group, MRC Clinical Sciences Centre, Faculty of Medicine, Imperial College, Hammersmith Campus, W12 0NN London, UK
[4]Departamento de Fisiología and Centro de Investigación en Medicina Molecular (CIMUS), Instituto de Investigación Sanitaria de Santiago (IDIS), Universidad de Santiago de Compostela, 15782 Spain
[5]Genomic Instability Group, Spanish National Cancer Research Centre (CNIO), Madrid, 28029 Spain
[6]These authors contributed equally to this work
*Correspondence: josema.torres@uv.es (J.T.), isabel.farinas@uv.es (I.F.)
http://dx.doi.org/10.1016/j.stem.2012.12.001

## SUMMARY

**In the adult brain, continual neurogenesis of olfactory neurons is sustained by the existence of neural stem cells (NSCs) in the subependymal niche. Elimination of the cyclin-dependent kinase inhibitor 1A (p21) leads to premature exhaustion of the subependymal NSC pool, suggesting a relationship between cell cycle control and long-term self-renewal, but the molecular mechanisms underlying NSC maintenance by p21 remain unexplored. Here we identify a function of p21 in the direct regulation of the expression of pluripotency factor Sox2, a key regulator of the specification and maintenance of neural progenitors. We observe that p21 directly binds a *Sox2* enhancer and negatively regulates Sox2 expression in NSCs. Augmented levels of Sox2 in *p21* null cells induce replicative stress and a DNA damage response that leads to cell growth arrest mediated by increased levels of $p19^{Arf}$ and p53. Our results show a regulation of NSC expansion driven by a p21/Sox2/p53 axis.**

## INTRODUCTION

Stem cells persist in the adult brain in two discrete niches, the subependymal zone (SEZ), which generates olfactory interneurons and callosal oligodendrocytes, and the neurogenic subgranular zone (SGZ) of the hippocampus. In the SEZ, in particular, glial fibrillary acidic protein (GFAP) and Nestin-expressing multipotential astrocytes with rather long cell cycles (B cells) appear to act as neural stem cells (NSCs). Activated, proliferative B cells produce transit-amplifying progenitor cells, which primarily differentiate into neurons (Zhao et al., 2008). These activated B cells can be isolated and grown in culture as neurospheres with mitogens epidermal growth factor (EGF) and/or basic fibroblast growth factor (bFGF); under these conditions, they exhibit self-renewal and the potential to clonally differentiate into neurons, astrocytes, and oligodendrocytes (Andreu-Agulló et al., 2009). Lifelong neurogenesis and expansion of multipotent cultures in vitro are a reflection of NSC self-renewal, an essential property of stem cell populations that integrates cell proliferation with the maintenance of an undifferentiated state. Self-renewal is regulated by cell-extrinsic signals, produced within endogenous stem cell niches, and intrinsic regulators. Among intrinsic modulators, transcription factors that are important to sustain stem cell developmental potential and modulators of the cell cycle status appear especially relevant (Orford and Scadden, 2008).

SOX transcription factors are characterized by an SRY box, a 79 amino acid high-mobility-group (HMG)-type DNA binding domain (Wegner, 2011). Closely related factors Sox1, Sox2, and Sox3 of the SoxB1 subfamily are expressed in most neural stem/progenitor cells and play a role in maintaining their undifferentiated state, albeit with some functional redundancy (Graham et al., 2003; Bylund et al., 2003; Bani-Yaghoub et al., 2006; Miyagi et al., 2008; Wegner, 2011). Sox2, in particular, is expressed at high levels in adult NSCs and is required for their self-renewal. A reduction in Sox2 levels results in a loss of GFAP-positive progenitor cells and deficient neurogenesis in the murine hippocampus (Ellis et al., 2004; Ferri et al., 2004; Favaro et al., 2009), and *SOX2* hemizygosity in humans associates with neurological phenotypes and hippocampal malformation (Sisodiya et al., 2006). In addition, *SOX2* expression is high in gliomas and *SOX2* silencing in glioblastoma tumor-initiating cells reduces their proliferation (Gangemi et al., 2009). Despite the relevant role of Sox2 in the regulation of normal and transformed NSCs, very little is known about the control of Sox2 expression in adult NSCs.

Sox2 is present in long-lived adult stem cells and is essential for the pluripotency of epiblast cells and embryonic stem cells (ESCs) (Wegner, 2011; Arnold et al., 2011). In line with this, Sox2 is one of the factors (together with Oct4/Klf4/c-Myc) that mediate the reprogramming of terminally differentiated somatic cells to a pluripotent state (Banito and Gil, 2010).

Please cite this article in press as: Marqués-Torrejón et al., Cyclin-Dependent Kinase Inhibitor p21 Controls Adult Neural Stem Cell Expansion by Regulating Sox2 Gene Expression, Cell Stem Cell (2013), http://dx.doi.org/10.1016/j.stem.2012.12.001



Reprogramming is highly improved by the ablation of different senescence effectors, indicating that senescence acts as a barrier for the completion of this process. In line with this, ectopic expression of pluripotency factors in fibroblasts can trigger senescence by upregulating the tumor suppressor p53 (also known as Trp53 in mice and TP53 in humans) and the cell cycle regulator p21 (also known as Cdkn1a and Cip1) (Banito and Gil, 2010; Blasco et al., 2011). Interestingly, cell cycling of adult murine NSCs is tightly regulated by p21, seemingly in a p53-independent manner (Kippin et al., 2005; Meletis et al., 2006). NSCs that are deficient in p21 exhibit increased cell cycle re-entry, leading to subsequent exhaustion of the NSC pool (Kippin et al., 2005), though the mechanisms involved in p21-dependent regulation of self-renewal are not understood.

Here we show that p21 directly binds to the Sox2 regulatory region 2 (SRR2) enhancer downstream of the *Sox2* gene and inhibits the expression of this gene in adult SEZ-derived NSCs. The loss of p21 results in increased levels of Sox2 leading to replicative stress (RS) that ultimately results in an arrest in stem cell growth that is dependent on the p53 and $p19^{Arf}$ tumor suppressors. Our results indicate that the modulation of Sox2 levels by p21 could be a regulatory mechanism to control the proliferation of NSC populations in the adult brain.

## RESULTS

### Sox2-Dependent Growth Arrest of p21-Deficient NSCs

Young p21-deficient mice exhibit increased numbers of long-term 2-bromo-5-deoxyuridine (BrdU)-retaining cells in the SEZ and yield more subependyma-derived neurospheres than wild-type littermates (Kippin et al., 2005). In agreement with the role of p21 as a cell cycle breaker in adult B NSCs, we observed in the SEZ of 2-month-old *p21*-null mice a higher proportion of GFAP/Nestin double positive (DP) cells (10.0% ± 2.6% versus wild-type values of 3.5% ± 0.5%; n = 3, $p < 0.05$) and GFAP/Nestin DP cells that were also positive for the cell proliferation marker Ki67 (Figures 1A and 1B). We also observed increased percentages of GFAP/Sox2 DP cells (44.3% ± 2.0% versus wild-type values of 32.0% ± 2.7%; n = 3, $p < 0.05$) and of GFAP/Nestin DP cells that were also positive for Sox2 (Figures 1B and 1C).

The levels of Sox2 in individual cells are variable among the proliferating cells of the SEZ (Ferri et al., 2004; Ellis et al., 2004) and, indeed, we could observe GFAP/Sox2 DP cells with differing, high or low levels of Sox2 protein (Figure 1C). Intriguingly, the lack of p21 resulted in increased proportions of GFAP-positive cells with high levels of Sox2 protein compared to those of wild-type controls (Figures 1B-1E), suggesting a potential regulation of Sox2 levels by p21. Moreover, *p21*-null mice showed an increase in the percentages of Ki67-positive cells within the GFAP/$Sox2^{low}$ population but a decrease in the proportion of Ki67-positive cells among the GFAP/$Sox2^{high}$ population (Figures 1E and 1F). These data suggested that, whereas more GFAP-positive B-type cells are cycling in the absence of p21, a fraction of GFAP/$Sox2^{high}$ cells may be arresting.

Expression of p21 is indispensable for the long-term self-renewal of adult NSCs and *p21*-null NSCs have a proliferative advantage at young ages that leads to their accelerated consumption during aging (Kippin et al., 2005). The exhaustion phenotype is readily manifested in vitro, when cells from the SEZ are grown and passaged as clonal neurospheres under mitogenic stimulation with EGF and FGF2. In fact, *p21*-null mice yield higher numbers of neurospheres than wild-type controls, but the cultures exhibit an eventual loss of neurosphere-forming ability (Kippin et al., 2005). In agreement with these findings, we observed that, in comparison with the wild-type litter mates, cellular cultures derived from the SEZ of young p21 mutant mice yielded higher numbers of primary neurospheres, which produced increased numbers of passage (P) 1 neurospheres that incorporated more BrdU (Figure 2A and Figures S1A and S1B available online), but fewer secondary neurospheres after P2 (95 ± 3 out of 500 cells plated in wild-type versus 69 ± 8 in *p21* mutant cultures; n = 4, $p < 0.01$) when the cells were seeded at 2.5 cells/μl to preserve the clonality of the assay (Ferrón et al., 2007). The results indicated defects in self-renewal that could be observed at the level of a single neurosphere.

Because large neurospheres appear to be more self-renewing (Kippin et al., 2005; Andreu-Agulló et al., 2009), we selected neurospheres that were above 100 μm in diameter after 7 days in vitro for analysis at each passage (Figures 2A and 2B). These neurospheres always produced both large and small clones, whereas further culture of the smaller neurospheres gave rise only to spheres below the 100 μm cut-off (data not shown). Relative to those from wild-type controls, primary cultures from *p21*-deficient mice yielded increased numbers of large P1 neurospheres. However, these gave rise to neurospheres that displayed reduced BrdU incorporation without changes in survival (Figures S1A–S1C), suggesting that the proliferation of p21-deficient NSCs was impaired during passaging. With passaging, the proportion of large neurospheres rapidly declined, reaching exhaustion as early as P3, whereas the proportion of neurospheres <100 μm increased (Figure 2C). This analysis indicated a cell growth arrest of self-renewing NSCs in the absence of p21 and provided us with a system to examine molecular changes underlying the exhaustion phenotype.

Using this system, we investigated Sox2 expression and observed a specific upregulation of its mRNA (2.70 ± 0.12-fold increase, n = 3; $p < 0.01$) in P2 large mutant neurospheres by quantitative real-time polymerase chain reaction (qPCR) (Figure 2D). Confocal and quantitative fluorescence microscopy also revealed a higher proportion of *p21*-null cells positive for Sox2 and increased Sox2 protein levels per nucleus in *p21*-deficient cultures (Figures 2E and S1D). These results indicated that the upregulation of Sox2 in a *p21*-null background correlates with impaired NSC expansion also in vitro.

We then performed rescue experiments by infecting single cells obtained from P2-neurospheres with retroviruses carrying p21 in the transfer vector pMSCV2.2-GFP-IRES-p21 (pMigR1-p21). Re-expression of p21 rescued the proportion of large P3-neurospheres to that of wild-type levels (Figures 2F and 2G), indicating that the deficits are likely a direct result of the loss of p21 in adult NSCs, in agreement with a previous report that p21 loss has no apparent effects during fetal/early postnatal development (Kippin et al., 2005). Restoration of p21 levels in mutant cells and subsequent rescuing effects correlated with reduced Sox2 protein levels (Figure 2H). To test whether augmented levels of Sox2 were indeed responsible for the growth arrest, we knocked down Sox2 expression in *p21*-deficient

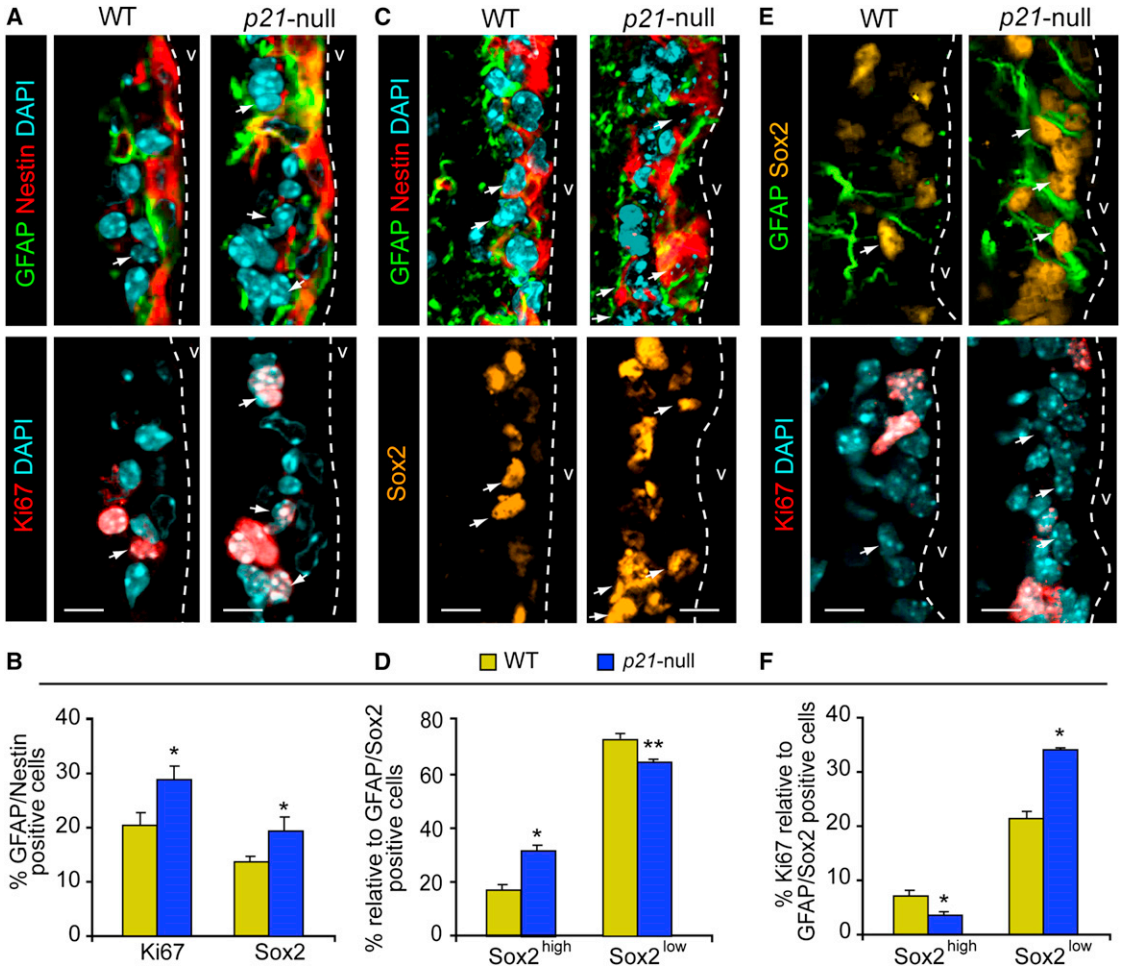


**Figure 1. Higher Levels of Sox2 in the SEZ of p21 Null Mice Negatively Correlate with B Cell Proliferation**

(A) GFAP (green) and Nestin (red) (top panels) and Ki67 (red) (bottom panels) in wild-type (WT) or *p21*-null mice.

(B) Percentages of Ki67-positive and Sox2-positive cells within the GFAP/Nestin DP cell population.

(C) GFAP (green) and Nestin (red) (top panels) and Sox2 (orange) (bottom panels) in WT or *p21*-null mice.

(D) Percentage of $Sox2^{high}$ and $Sox2^{low}$ cells within the GFAP/Sox2 DP cell population.

(E) GFAP (green) and Sox2 (orange) (top panels) and Ki67 (red) (bottom panels) in WT or *p21*-null mice.

(F) Percentage of Ki67-positive cells within the GFAP/$Sox2^{high}$ and GFAP/$Sox2^{low}$ cells.

DAPI is used as nuclear counterstaining. The dashed white line indicates the lateral ventricle (v) limit. White arrows indicate triple positive cells. All images are confocal 2 μm thick optical sections. Data are shown as mean values ± SEM (*$p < 0.05$; **$p < 0.01$). Scale bars: in (A), (C), and (E), 10 μm. See also Figure S1 and Table S1.

NSCs using short-hairpin RNAs (pRS-shRNA-Sox2; Banito et al., 2009). Knockdown of Sox2 in wild-type cells leading to about 50% reduction of *Sox2* mRNA levels slightly reduced the yield of large P3-neurospheres. Remarkably, the reduction of Sox2 in *p21* null NSCs rescued the numbers of large P3-neurospheres to those of wild-type levels (Figures 2F, 2G, and 2I), an indication that p21 maintains self-renewal by negatively regulating Sox2 expression.

## The CKI p21 Regulates Sox2 Gene Expression

It has been shown that p21 can modulate transcription by direct association with transcription factors/coactivators at specific promoters in a cell-cycle-independent way (Dotto, 2000; Devgan et al., 2005; Besson et al., 2008). Consistent with the possibility that p21 might directly regulate the expression of *Sox2*, a 2.5-fold increase in the expression of p21 over endogenous levels led to a 70% reduction in *Sox2* mRNA by qPCR (Figure S2A). Expression of *Sox2* in ESCs and NSCs is under the control of two enhancer regions, SRR1 and SRR2 (Figure 3A) and reporter analysis in vivo indicates that the SRR2 element (located 3 kbp downstream of the *Sox2* gene) functions to upregulate *Sox2* expression in fetal NSCs and B cells of the adult SEZ (Miyagi et al., 2004, 2006). Cytometry-based assays for the fluorescent product of the Venus reporter gene driven by a herpes simplex virus thymidine kinase basal promoter (positions 109 to 51) and the SRR2 region (positions 3641 to 4023) (Miyagi et al., 2004) in wild-type NSCs indicated that conucleofection with a pcDNA3.1-p21 inhibited transcription from the SRR2-TK-Venus reporter (45% ± 12% fluorescence intensity relative to empty vector) while expression from the control

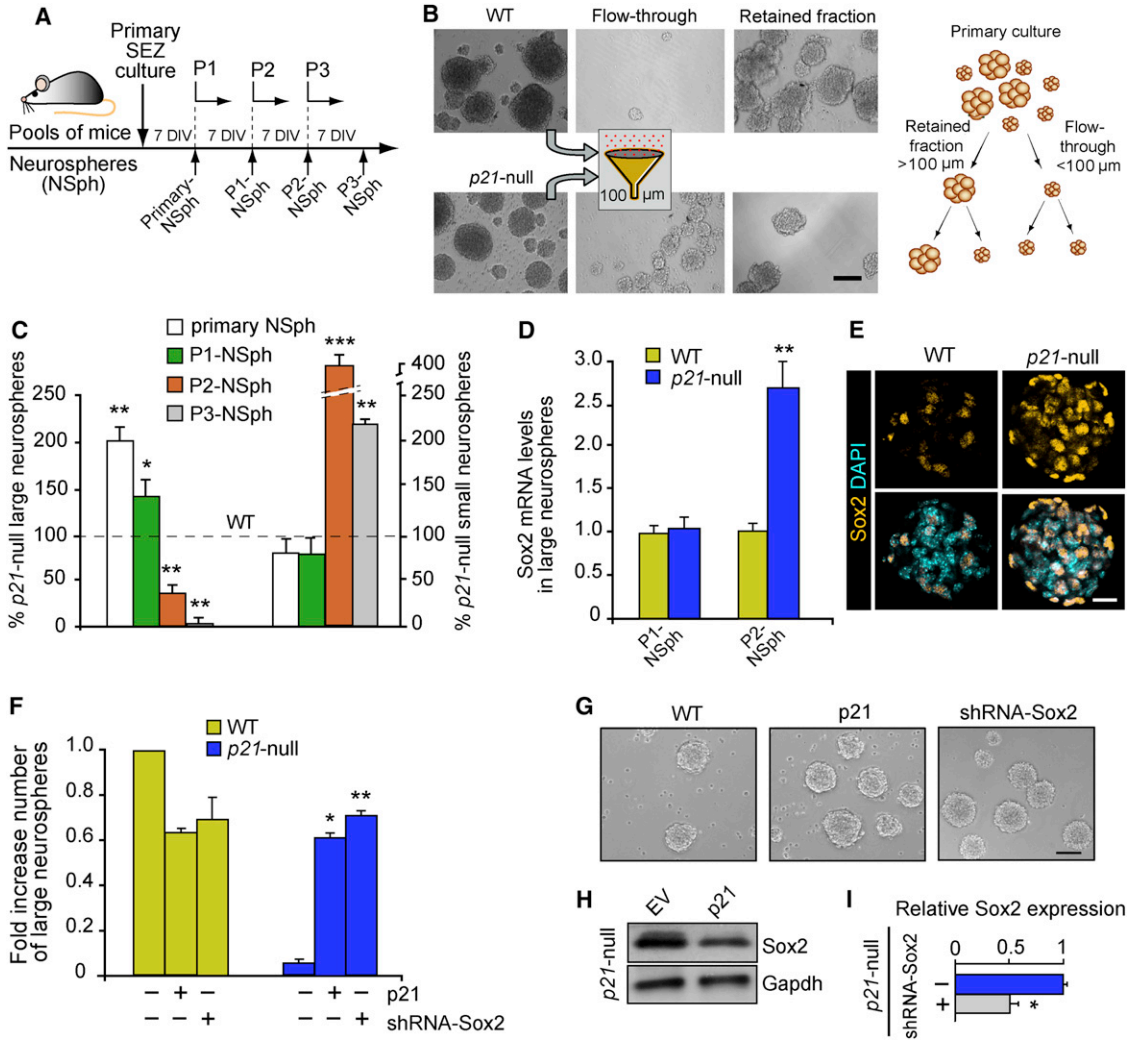


**Figure 2. Growth Arrest of p21-Deficient NSCs Is Sox2 Dependent**

(A) Schematic of the neurosphere (NSph) culture along the different passages (P).

(B) Phase contrast images of P2-NSphs from wild-type (WT) or *p21*-null mice (upper and lower panels, respectively) selected by size (left). Schematic depicting the size-based selection of the cultures is shown at right.

(C) With passaging, *p21*-deficient NSC cultures undergo a premature growth arrest (left axis) that is associated with a decrease in the diameter of the NSphs (right axis), relative to cultures from wild-type mice (100%, dashed line) (n = 5).

(D) Sox2 mRNA levels by qPCR, showing an increase of endogenous Sox2 expression in P2, but not P1, p21-deficient NSphs that correlates with reduced clonogenicity of large NSphs.

(E) Sox2 (orange) in WT and *p21*-null NSCs. DAPI is used as nuclear counterstaining.

(F) Expression of p21 or knockdown of *Sox2* rescues the growth arrest exhibited by *p21*-deficient NSCs (n = 3).

(G) Phase contrast images of p21-deficient neurospheres infected with retroviruses carrying an empty vector (EV), a p21 cDNA (p21), or a Sox2 shRNA.

(H) Immunoblot for Sox2 protein in *p21*-null cells transduced with empty vector (EV) or p21.

(I) Relative Sox2 expression by qPCR in *p21* null cells transduced with EV or a specific shRNA.

Scale bars: in (E), 20 µm; in (B) and (G), 100 µm. Data are shown as mean ± SEM of the indicated number of the experiments (n) (*p < 0.05; **p < 0.01; ***p < 0.001). See also Figure S1 and Table S1.

TK reporter was unchanged (Figure 3B). In addition, we observed a significant specific activation of the SRR2 reporter in *p21*-null cells when compared to that of wild-type controls (2.51 ± 0.05-fold increase in mean fluorescence intensity; Figure 3C), indicating that p21 can regulate the SRR2 enhancer activity.

To test the possibility of a direct interaction of p21 with the SRR2 enhancer, we performed chromatin immunoprecipitation (ChIP) assays with anti-FLAG antibodies in chromatin isolated from neurospheres that had been infected with retroviruses bearing a GFP reporter, either empty (pMigR1) or containing a p21-FLAG cDNA. The levels of p21 mRNA and protein achieved by the retroviral infection of p21-deficient cells were similar to the physiological levels observed in wild-type cells (Figures 3D and 3E). Under these conditions, we observed specific binding of FLAG-tagged p21 to the SRR2 enhancer that was validated

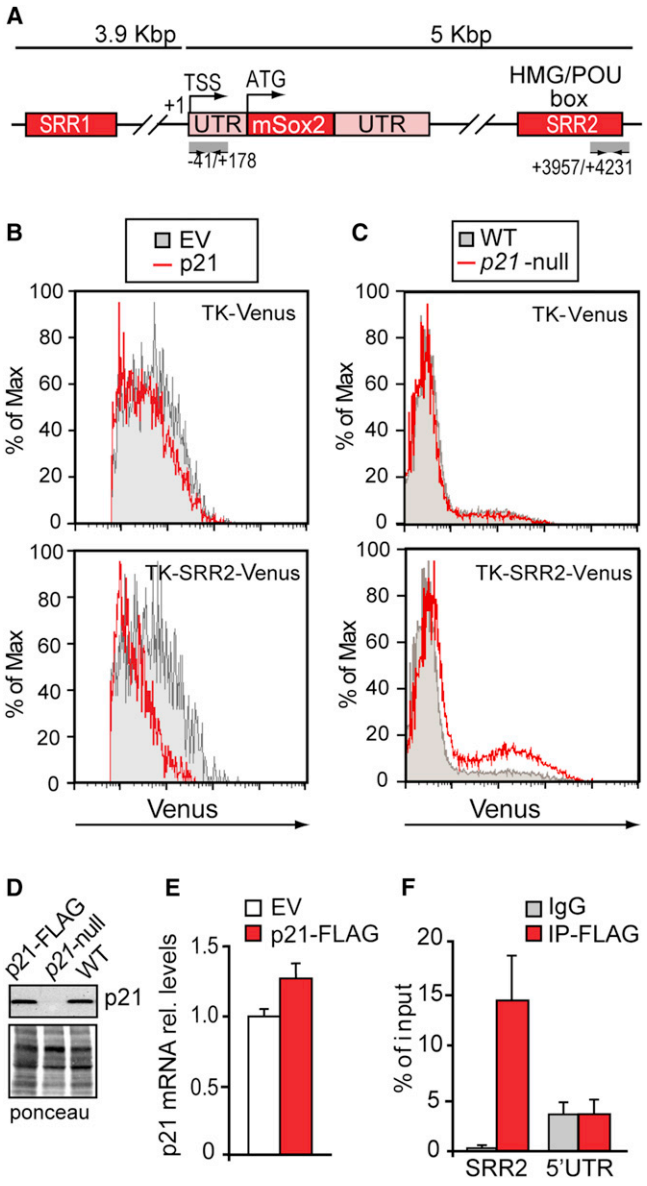


**Figure 3. p21 Inhibits Sox2 Gene Expression**

(A) Regulatory regions in the murine *Sox2* locus.

(B) Flow cytometric analysis of Venus expression in NSCs transfected with the indicated reporters in the absence or presence of recombinant p21; a representative experiment is shown (n = 2).

(C) Flow cytometric analysis of Venus expression in WT or *p21*-null NSCs; a representative experiment is shown (n = 2).

(D) Immunoblot showing the levels of p21 in *p21*-null NSCs, or wild-type NSCs left untreated (WT) or transduced with p21-expressing viruses (p21-FLAG). Ponceau staining of the membrane is shown as a loading control.

(E) Levels of p21 mRNA expression in WT NSCs infected with GFP (EV) or GFP-p21-FLAG-expressing viruses (n = 3).

(F) NSCs infected with FLAG-tagged p21-expressing viruses were subjected to ChIP assays with anti-FLAG or isotype control (IgG) antibodies. The graph shows the quantitation of p21 binding to the indicated regions of the *Sox2* gene by qPCR (n = 2).

Data are shown as mean ± SEM of the indicated number of the experiments (n) (*$p < 0.05$). See also Figure S2 and Tables S1 and S2.

by qPCR of immunoprecipitated chromatin fragments. Primers directed to a promoter region were used to confirm the binding specificity (Figure 3F). Moreover, ChIP analysis in cells of the c17.2 neural stem cell line with two different antibodies evidenced specific binding of endogenous p21 to the SRR2 enhancer in contrast to the promoter region tested (Figure S2B). These results indicate a direct role of p21 in the inhibition of the SRR2 enhancer in NSCs.

## Elevated Sox2 Levels Induce Senescence in Neurosphere-Forming Cells

NSCs isolated from neonatal mice require Sox2 to grow and self-renew (Favaro et al., 2009), but our results suggested that upregulation of Sox2 in adult NSCs might impair self-renewal. In pluripotent ESCs either a reduction or an increase in Sox2 levels can impair pluripotency and self-renewal (Kopp et al., 2008), suggesting that Sox2 levels should be kept within strictly regulated levels in stem cells. Moreover, overexpression of reprogramming factors results in increased proportions of cells displaying senescent features (Banito et al., 2009; Hong et al., 2009; Kawamura et al., 2009; Marión et al., 2009; Li et al., 2009; Banito and Gil, 2010). In agreement with this, we observed that overexpression of Sox2 in mouse embryonic fibroblasts (MEFs) caused a drastic reduction in cell proliferation, along with a 2-fold increase in the proportion of senescence-associated (SA)-β-galactosidase-positive cells (Figures 4A and S3A).

To investigate the role of increased levels of Sox2 in the regulation of adult NSCs features, wild-type cells were transduced with retroviruses carrying pMY-GFP or pMY-GFP-IRES-Sox2 and FACS-sorted cells were subjected to self-renewal and clonal multipotency assays. Cultures overexpressing Sox2 (45% increase relative to controls, as determined by immunoblot) showed a reduction in the number (53% ± 11% decrease, $n = 5$, $p < 0.05$) and size (57 ± 6 versus 96 ± 8 μm in diameter; $n = 5$, $p < 0.05$) of secondary neurospheres when compared with the GFP controls (Figures 4B and 4C). Moreover, when these neurospheres were individually picked and allowed to differentiate for 7 days and evaluated for the presence of the three neural lineages (oligodendrocytes, astrocytes, and neurons) by immunofluorescence, we found that overexpression of Sox2 impaired NSC potentiality, reflected in a significant increase in the proportion of unipotent, astrocyte-only clones at the expense of tripotent clones (Figures 4B and 4D). Together, these results indicated that elevated levels of Sox2 restrain self-renewal of adult NSCs, reducing their neurosphere-forming potential and multilineage differentiation. The increment in Sox2 levels was not associated with increased apoptosis (Figures S3B and S3C) but with a higher proportion of cells exhibiting SA-β-galactosidase staining (Figure 4B). These results indicated that reduced stem cell frequency and self-renewal potential following overexpression of Sox2 were likely the result of cell growth arrest/senescence in neurosphere-forming cells.

## Increased Levels of DNA Damage in *p21*-Null Cells Are Associated with Sox2 Overexpression

Senescence can be the result of replicative exhaustion or can be elicited in response to stresses such as DNA damage (Collado et al., 2007). In this regard, Sox2 overexpression in wild-type NSCs resulted in significantly higher percentages of cells

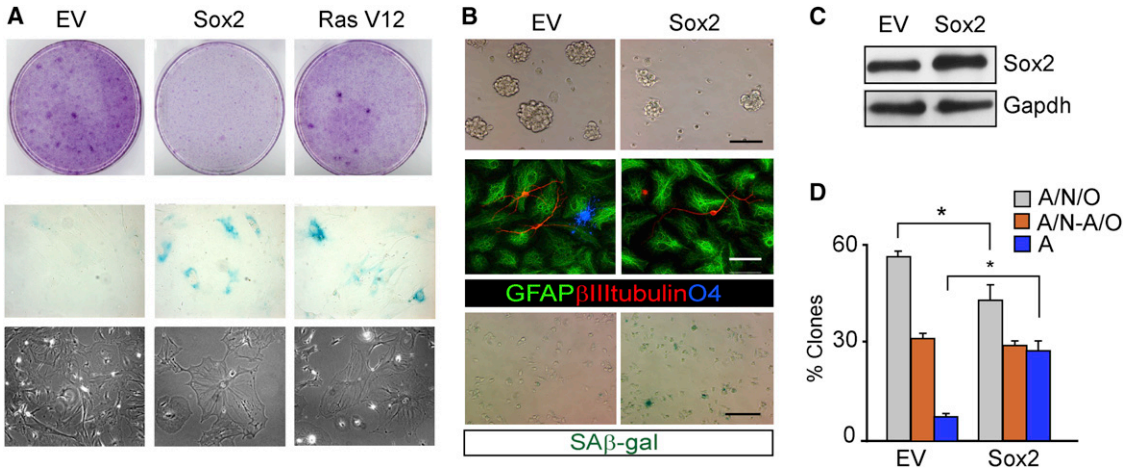


**Figure 4. Sox2 Overexpression in NSCs Induces Senescence**

(A) MEFs were infected with empty vector (EV) or constructs encoding the indicated factors. Cells were selected for 7 days and used for crystal violet (upper panels) or SA-β-galactosidase stainings (middle panels). Phase-contrast images of the cells at the end of the selection are shown (lower panels). Oncogenic Ras V12 is used as a positive control.

(B) NSCs were infected with EV or Sox2. From the top: expression of Sox2 reduces the number and size of secondary neurospheres (phase-contrast; upper panels), impairs multipotency (immunofluorescence with the indicated antibodies; middle panels), and induces senescence (SA-β-galactosidase; lower panels).

(C) Sox2 protein levels in the NSCs infected with EV or Sox2.

(D) Quantitation of the differentiation potential of the infected NSCs in (B) (n = 3).

Data are shown as mean ± SEM of the indicated number of the experiments (n) (*$p < 0.05$). Scale bars: in (B), upper panels 100 μm; middle panels 30 μm; lower panel 50 μm. See also Figure S3 and Table S1.

immunopositive for the form of histone H2AX phosphorylated in serine 139 (γH2AX), a widespread marker of DNA damage and RS (Figures 5A–5C). Since γH2AX can be phosphorylated at stalled replication forks even in the absence of DNA breakage, we also analyzed the presence of nuclear foci of 53BP1, which specifically marks sites of chromosome breaks. Forced expression of Sox2 led to a 2-fold and 5-fold increase in the percentage of γH2AX-positive or 53BP1 foci-containing cells, respectively, relative to those of the controls (Figures 5C and S4). Oncogene-induced DNA breaks that promote senescence are thought to be initiated by RS, which, if persistent, can lead to chromosomal breakage. Indeed, Sox2-transduced cultures contained more cells exhibiting single-stranded (ss) DNA-binding replication protein A (RPA32) foci typically associated with stalled DNA replication forks and RS (Figures 5B and 5C).

Similarly to Sox2-overexpressing cells, we observed higher proportions of cells with RPA32- and 53BP1-positive foci and γH2AX in *p21* null cultures than in wild-type controls (Figures 5D–5F), an indication of augmented RS and DNA damage. Reintroduction of a full-length p21 cDNA restored the increased percentages of 53BP1-positive cells to wild-type levels (Figure 5F). Since our results indicated that lack of p21 results in genomic instability, we next investigated whether this correlated with the deregulation of Sox2 expression. Indeed, 70% ± 15% of the Sox2-positive *p21*-null cells were also positive for γH2AX, suggesting that increased Sox2 levels could be behind the instability found in p21-deficient NSCs.

Analyses in vivo showed a general increase in the proportion of GFAP-positive cells that were also positive for γH2AX (59.5% ± 3.9% versus wild-type values of 44.5% ± 2.9%; $n = 6$, $p < 0.05$) or RPA foci (56.1% ± 6.2% versus wild-type values of 30.4% ± 3.3%; $n = 3$, $p < 0.05$) and an increase in the percentage of γH2AX-positive cells within the GFAP/Sox2$^{high}$ population in *p21* null mice (Figures 5G and 5H). It has been reported that H2AX can also be phosphorylated by kinases of the PIKK family in response to GABA signals that are naturally produced in the subependymal niche, suggesting that activation of a H2AX signaling pathway may represent one mechanism restricting NSC proliferation under physiological conditions (Fernando et al., 2011). However, 80.8% ± 3.8% of the γH2AX/GFAP DP cells in the SEZ of p21-deficient mice presented additional evidences of DNA breakage such as 53BP1 foci, in contrast to a wild-type value of 37.3% ± 4.2% ($n = 3$, $p < 0.001$). To provide formal genetic proof that the origin of the DNA damage found on *p21*-null mice was linked to RS, we focused on the Chk1 kinase, which coordinates the RS response, and took advantage of a recently generated mouse strain carrying an extra allele of Chk1 (*Chk1$^{Tg}$*), which is selectively protected from RS (Toledo et al., 2011; López-Contreras et al., 2012). Importantly, the introduction of the *Chk1$^{Tg}$* on the *p21* null background diminished the percentage of GFAP/Sox2-positive cells showing γH2AX phosphorylation (Figures 5G and 5H). All together, these results support the idea that Sox2 overexpression in p21-deficient NSCs leads to RS and subsequent DNA breakage.

## DNA Damage Checkpoint Activation in *p21*-Null Is Sox2 Dependent

Senescence is controlled by the tumor suppressor p53 and by p16$^{Ink4a}$ (p16) and p19$^{Arf}$ (encoded by alternative reading frames of the *Ink4a/Arf* locus, also known as *Cdkn2a*) (Collado et al., 2007; Banito and Gil, 2010). Oncogene-induced stress results in increased production of p19$^{Arf}$, which, in turn, raises p53 levels by inhibiting MDM2, the E3-ubiquitin ligase mainly responsible

for its degradation (Collado et al., 2007). In this regard, forced expression of pluripotency factors induces the accumulation of p53, p16, and/or $p19^{Arf}$ proteins in MEFs and $p19^{Arf}$ acts as the main barrier to reprogramming in murine cells (Li et al., 2009; Banito and Gil, 2010). In fact, we observed that overexpression of Sox2 in wild-type, but not *p53*-deficient, MEFs led to a cell growth arrest associated with an increase in the levels of the products of the *Cdkn2a* gene (Figures 6A and S5A and S5B). We also observed an accumulation of the p53 protein in NSCs in response to increased levels of Sox2, and, more importantly, Sox2 overexpression did not affect the self-renewal of *p53* null NSCs (Figures 6B and 6C). Together, these findings demonstrated that expression of Sox2 above physiological levels induces cell growth arrest in a p53-dependent manner.

It has been reported that oncogene-dependent RS can induce a DSB-initiated DNA damage response (DDR) within a single cell cycle (Bartkova et al., 2006; Di Micco et al., 2006). In agreement with this, oncogene-induced senescence could be bypassed by depletion of the DSB-responsive kinase ATM (Shiloh, 2003). Since DSB markers such as 53BP1 foci are elevated on p21-deficient NSCs, to determine whether the DDR was involved in the growth arrest induced by Sox2 overexpression, we tested the effect of KU55933, a specific pharmacological inhibitor of ATM, in the ability of GFP and GFP-Sox2 overexpressing NSCs to form neurospheres. Despite a limited toxicity of the drug, Sox2-overexpressing cultures treated with 1 μM KU55933 yielded neurosphere numbers similar to those of GFP controls (Figure 6C). Furthermore, permanent inhibition of the ATM kinase by continual treatment with the drug rescued the yield of P3-large mutant neurospheres to wild-type values (wild-type: 33.1 ± 5.2; *p21* null: 6.7 ± 1.2; *p21*-null treated with KU55933: 29.0 ± 0.1; n = 2–7).

Expression analysis by qPCR indicated that, while there was no change in the levels of *p16* between genotypes, the levels of $p19^{Arf}$ mRNA went up by 2-fold in *p21*-null NSCs (Figure 6D). In addition, quantitative microscopy revealed a higher amount of $p19^{Arf}$ and p53 proteins per nucleus in *p21*-null NSCs compared to those of wild-type NSCs (Figure 6E). Retroviral delivery of *p16/p19*$^{Arf}$ or *p53* shRNAs to *p21*-null P2 cells did not modify the proportions of cells positive for γH2AX (38.3% ± 2.3% empty vector; 30.0% ± 4.0% shRNA-*p16/19*$^{Arf}$; 32.6% ± 3.2% shRNA-*p53*; n = 3) but restored the yield of large P3-neurospheres to wild-type levels (Figure 6F). Therefore, overexpression of Sox2 in p21-deficient NSCs triggers a p53-dependent cell growth arrest that could be initiated by the DDR and/or the induction of $p19^{Arf}$ expression.

We next sought to determine whether the increase in DNA damage markers was causally linked to Sox2 overexpression. Remarkably, the proportion of γH2AX-positive cells was decreased to wild-type values upon reduction of Sox2 levels in vitro by shRNA delivery (Figure 7A), suggesting that increased Sox2 activates the DDR in a similar fashion to the aberrant expression of oncogenes.

In order to analyze whether increased levels of Sox2 were also at the basis of the phenotypes observed in the *p21*-null mice in vivo, we crossed *p21* knockout mice with *Sox2* heterozygous mice and analyzed the offspring for DNA damage and RS markers in the SEZ. We observed that mice with reduced levels of Sox2 (*p21* null/*Sox2*-het; Figure S7) showed reduced levels of DNA damage markers and fewer GFAP-positive cells or GFAP/Nestin DP cells that were also positive for γH2AX or 53BP1 foci just by visual examination (Figure 7B). The signs of RS in *p21*-null mice, determined by the presence of RPA32 foci in GFAP/Nestin cells, also appeared alleviated in a *Sox2* heterozygous background (Figure 7C). Interestingly, DCX-positive neuroblasts derived from GFAP-positive B cells also displayed signs of RS in *p21*-null mice, which were reduced to wild-type levels in *p21*-null/*Sox2*-het mice (Figure 7D). The quantitations showed that reduction of Sox2 levels in a *p21*-null background indeed decreased the percentages of GFAP/γH2AX DP cells with 53BP1 foci, and the percentages of GFAP/Nestin DP cells and DCX-positive neuroblasts that were also positive for RPA32 foci, to wild-type levels (Figures 7E and 7F). In conclusion, the results presented here indicate that p21 preserves integrity of the NSC genome by finely modulating the levels of Sox2.

## DISCUSSION

The Cip/Kip p21 is a well-known cell cycle regulator and acts as a molecular break inducing a permanent cell cycle arrest (senescence) in response to DNA damage and p53 activation in most primary cells (Besson et al., 2008). Interestingly, p21 appears to mediate a distinct cellular response in stem cell populations. In NSCs and hematopoietic stem cells (HSCs), cell cycle restriction by p21 appears to be critical for self-renewal, as *p21*-deficient NSCs and HSCs proliferate more actively but become consumed over time (Kippin et al., 2005; Orford and Scadden, 2008). Still, the molecular mechanisms by which p21 regulates stem cell pools remain largely unknown. Our data support a model in which p21 can regulate NSC self-renewal, at least in part by repressing *Sox2* gene expression.

We show that p21 associates to the Sox2 enhancer SRR2 and represses *Sox2* gene expression. It has been reported that p21 does not bind directly to regulatory elements but can act as a repressor through binding to transcription factors, such as E2F1, c-Myc, or STAT3 (Dotto, 2000; Devgan et al., 2005). Recent data has indicated that p27, another member of the Cip/Kip subfamily of CKIs, also acts as a transcriptional repressor through binding to p130-E2F4 complexes; bound p27 is needed for the subsequent recruitment of mSin3A, a core protein of a corepressor HDAC1/HDAC2 histone deacetylase complex (Pippa et al., 2012). Although p21 can interact with E2F-containing complexes, expression of p130 and E2F4 is very low in our proliferating neurospheres and, moreover, p21 does not appear to be required for the binding of mSin3A to the SRR2 enhancer (data not shown), suggesting that p21 actions on *Sox2* transcription in NSCs likely depend on a different molecular mechanism. The specific activity of SRR2 in fetal NSCs is specified mainly by the Sox2 protein itself with the contribution of POU-domain proteins such as Brn-1, Brn-2 and Brn-4 or Oct6, in a way similar to the regulation of this enhancer in embryonic cells by Oct3/4-Sox2 complexes (Miyagi et al., 2004). Therefore, further work will be necessary to address whether interactions of p21 with any of these transcriptional regulators underlie its role in the repression of Sox2 in NSCs.

The work presented here also indicates that (1) in response to mitogenic stimuli, p21-deficient NSCs undergo cell growth arrest

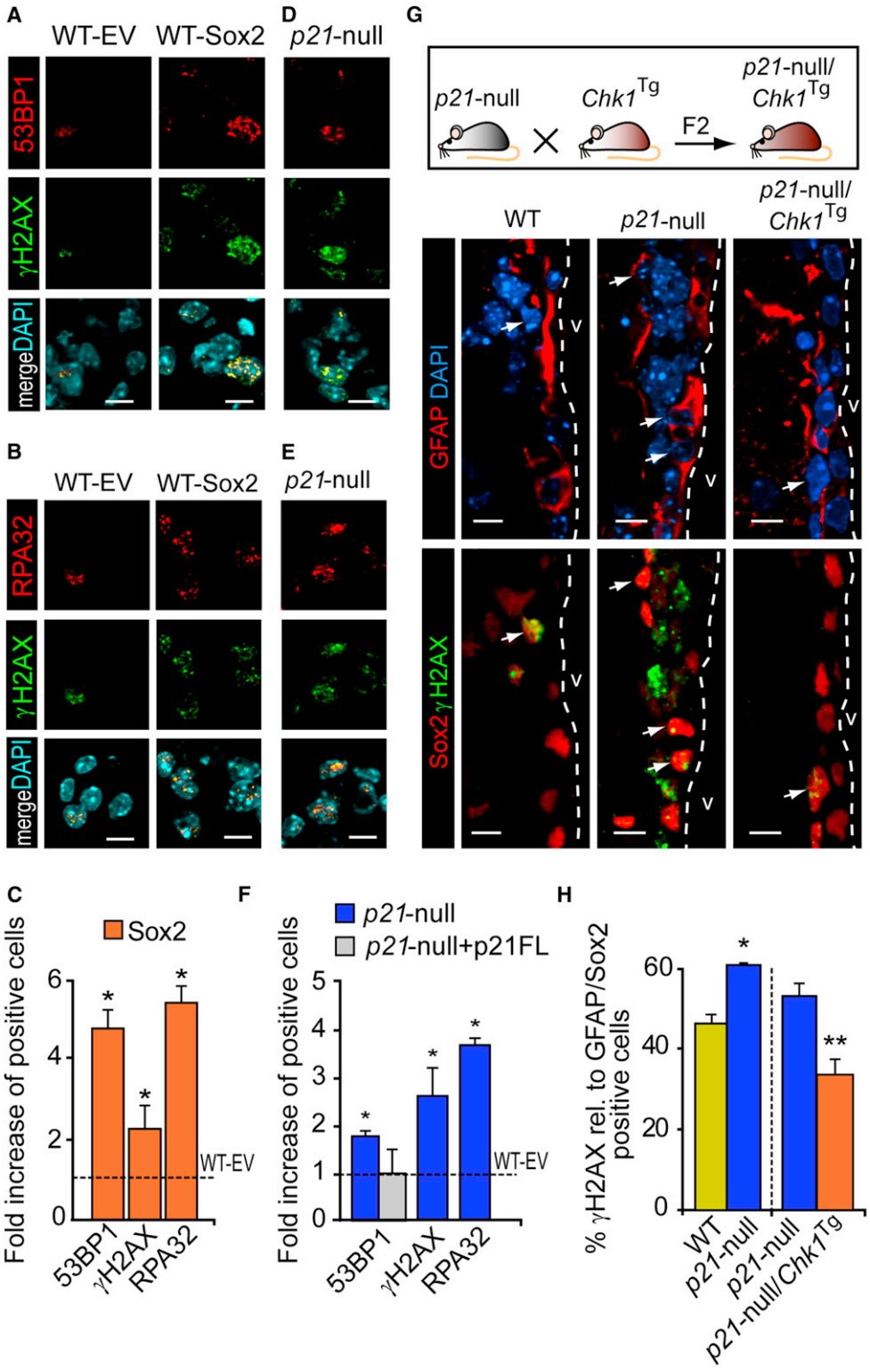


**Figure 5. Genomic Instability in p21-Deficient NSCs Is Associated with Sox2 Deregulation**

(A) Examples of Sox2-transduced NSCs showing increased immunostaining for γH2AX (green) and 53BP1 (red) relative to empty vector (EV) cells.

(B) Examples of Sox2-transduced NSCs showing increased immunostaining for γH2AX (green) and RPA32 (red) relative to EV cells.

(C) Quantitation of 53BP1, γH2AX, and RPA stainings in NSCs overexpressing Sox2 relative to EV-transduced cells (dashed line) (n = 3).

(D) Examples of *p21*-null cells showing increased immunostaining for γH2AX (green) and 53BP1 (red) relative to WT cells.

(E) Examples of *p21*-null cells showing increased immunostaining for γH2AX (green) and RPA32 (red) relative to WT cells.

*(legend continued on next page)*

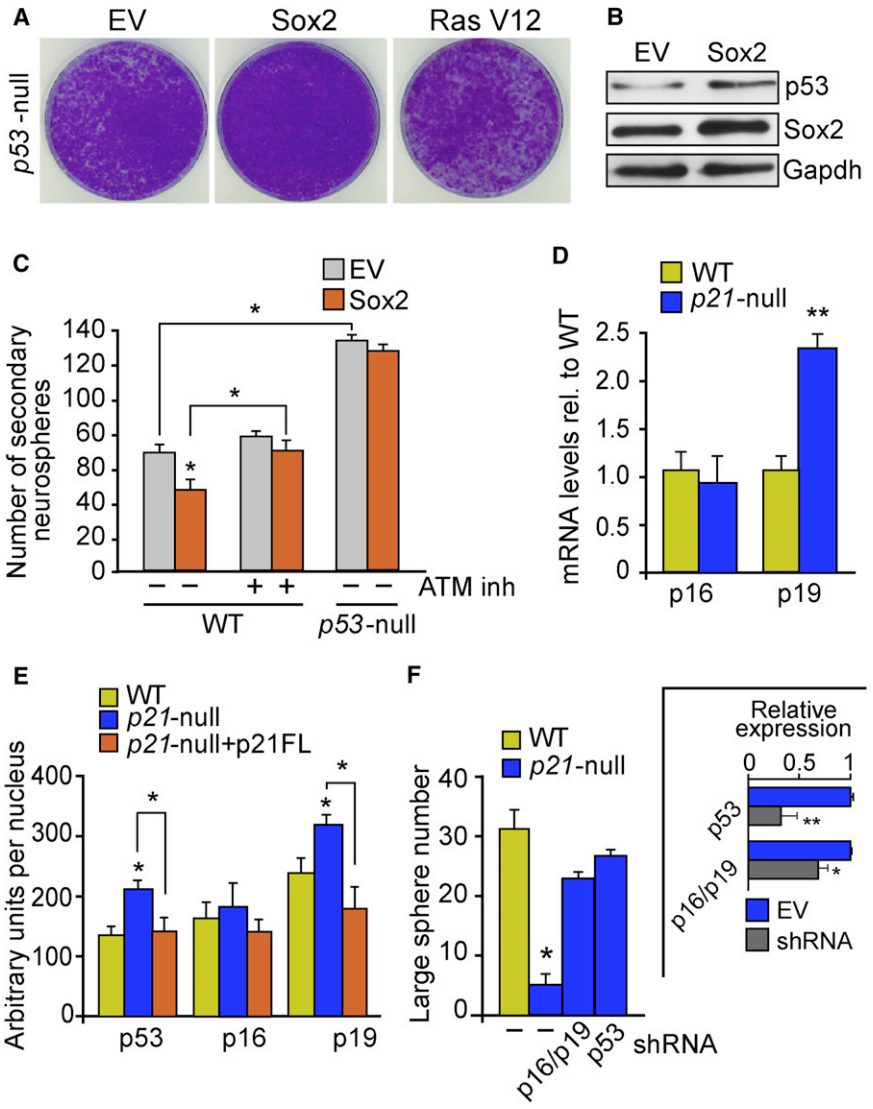


**Figure 6. DNA Damage Checkpoint Activation in p21-Null and Sox2-Overexpressing Cells**

(A) Crystal violet staining of murine *p53*-null MEFs transduced with empty vector (EV) or constructs encoding the indicated factors. Sox2 overexpression does not induce cellular senescence in the absence of p53. Oncogenic Ras V12 is used as a positive control.

(B) Sox2 overexpression in NSCs induces an increase in p53 protein levels.

(C) Retroviral expression of Sox2/GFP decreases the number of secondary neurospheres in WT, but not in *p53*-null, cultures. Treatment of Sox2/GFP-transduced cells with the ATM inhibitor KU55933 restored neurosphere formation to the levels found in GFP (EV)-transduced cells (n = 3).

(D) Assessment in WT or *p21*-null NSCs of *p16* and $p19^{Arf}$ mRNA levels by qRT-PCR (n = 3).

(E) Levels of immunostaining for p16, $p19^{Arf}$, and p53 in the nuclei of WT and *p21*-null cells, as measured by quantitative fluorescence microscopy (n = 3).

(F) p21-deficient neurospheres were transduced with control (–), p53, or p16/$p19^{Arf}$ shRNAs. The graph shows the rescue of the growth arrest observed in *p21*-deficient NSCs by knocking down *p16/19* or *p53*. The inset shows the knockdown efficiency of the indicated shRNA constructs by qPCR analysis. Data are shown as mean ± SEM of the indicated number of the experiments (n) (*$p < 0.05$). See also Figure S5 and Tables S1 and S2.

and exhibit signs of DNA damage that are reminiscent of RS and can, therefore, be alleviated by expression of an extra copy of Chk1; (2) Sox2 expression in NSCs is repressed by p21 and this correlates with a direct binding of p21 to the Sox2 enhancer; and (3) Sox2 depletion limits the damage that is observed in p21-deficient NSCs, both in vitro and in vivo. The results suggest a model whereby the repression of Sox2 by p21 is essential for maintaining a proper regulation of cell-cycle transitions in NSCs. In the absence of p21, Sox2 overexpression would allow a promiscuous entry in S-phase and therefore RS, which would ultimately limit NSC clonogenic potential. The mechanism by which NSCs undergo p53-mediated senescence in the absence of p21 is still unclear. It has been reported that p53 can induce cell growth arrest in the absence of p21 by increasing the expression of the genes encoding for Gadd45 and 14-3-3 proteins sigma (Taylor and Stark, 2001). However, we could not detect an increase in the expression of these genes in *p21* null NSCs (data not shown), suggesting that p53 may act in combination with yet other pathways to induce a growth arrest.

Normal stem cells are known to accumulate DNA damage during successive replication rounds that, in the end, compromises stem cell function (Rossi et al., 2007; Nijnik et al., 2007). Moreover, several lines of evidence suggest that stem cells demand an especially tight control of replication to prevent replicative damage. First, ESCs and iPSCs accumulate copy number variations (CNVs) upon serial culture (Närvä et al., 2010; Laurent et al., 2011), a type of genomic aberrations that are hallmarks of RS. Second, previous evidence exists to suggest that enhanced expression of stemness factors, including Sox2, in somatic cells

(F) Bar graph showing the quantitation of 53BP1, γH2AX, and RPA32 stainings in *p21*-null cells relative to WT-EV (dashed line) cells and of 53BP1 in *p21*-null NSCs re-expressing p21 (p21 null+p21FL) (n = 3).

(G) SEZ sections from WT mice, *p21*-null mice, or *p21-null;Chk1*$^{Tg}$ stained with the indicated antibodies. Triple positive cells are indicated by white arrowheads.

(H) Bar graph showing the proportions of GFAP/Sox2 DP cells that are also γH2AX positive in the SEZ of *p21*-null and WT mice and in the SEZ of *p21*-null;WT and *p21*-null;*Chk1*$^{Tg}$ mice (n = 3 animals per genotype).

All in vivo images are confocal 2 μm thick optical sections. Data are shown as mean ± SEM of the indicated number of the experiments (n) (*$p < 0.05$; **$p < 0.01$). Scale bars: in (A), (B), (D), and (E), 10 μm; in (G), 10 μm. See also Figure S4 and Table S1.

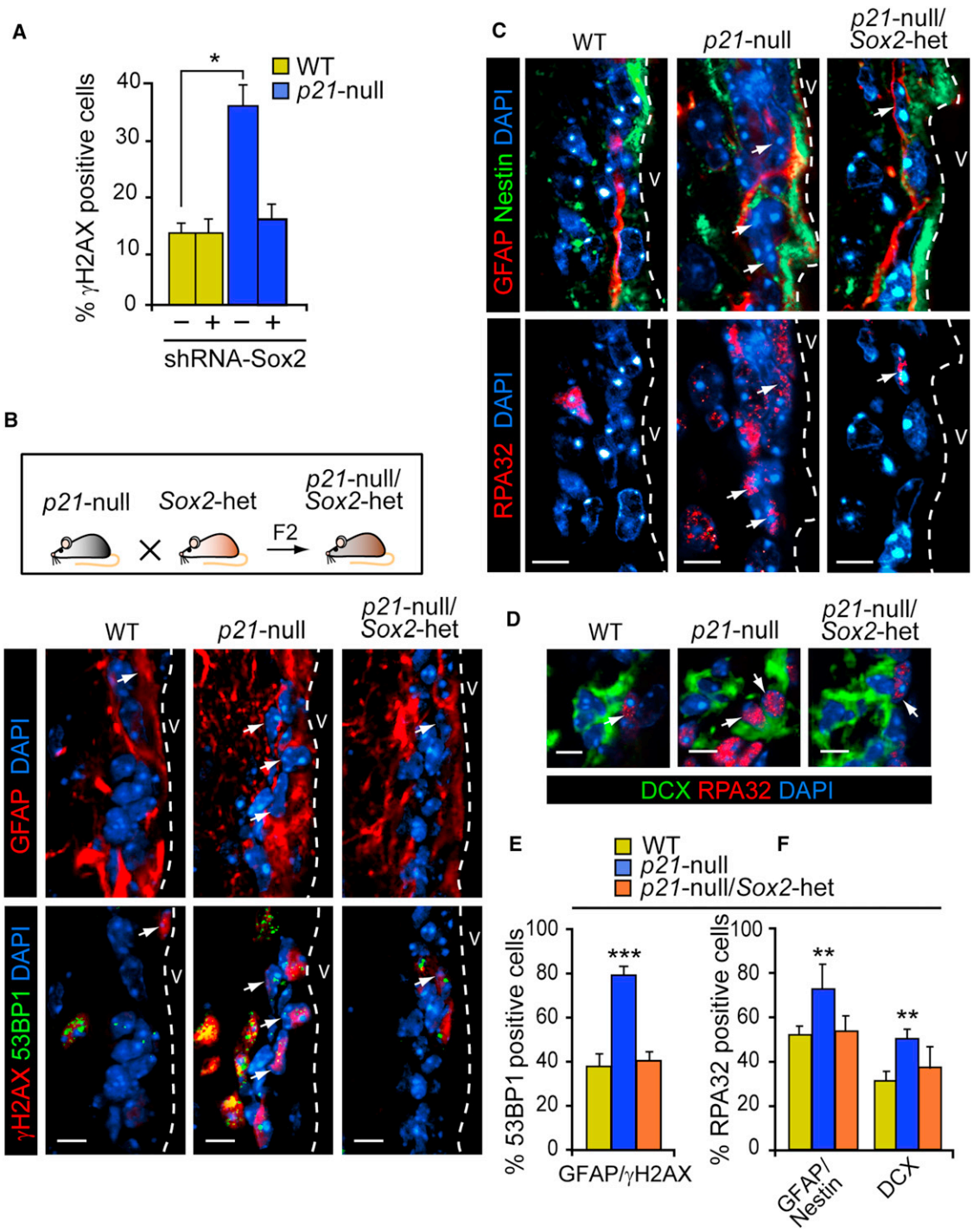


**Figure 7. Genomic Instability in p21-Null Cells Can Be Restored by Reduction of Sox2 Levels**

(A) Lack of p21 leads to an increase in γH2AX staining, which is rescued by Sox2 knockdown in neurosphere cells (n = 3).

(B) GFAP (red), γH2AX (red), and 53BP1 (green) in WT, *p21*-null, or *p21*-null/*Sox2*-het mice.

(C) GFAP (red), Nestin (green), and RPA32 (red) in WT, *p21*-null, or *p21*-null/*Sox2*-het mice. White arrows indicate triple positive cells in (B) and (C).

(D) DCX (green) and RPA (red) in WT, *p21*-null, or *p21*-null/*Sox2*-het mice. White arrows indicate DP cells.

(E) Graph showing the proportions of γH2AX and GFAP DP cells that are also positive for 53BP1 in WT, *p21*-null, or *p21*-null/*Sox2*-het mice (n = 3).

(F) Graph showing the proportions of Nestin and GFAP DP cells (left bars) and of DCX-positive neuroblasts (right bars) that are also RPA32 positive in WT, *p21*-null, or *p21*-null/*Sox2*-het mice (n = 3). DAPI (blue) is used for counterstaining.1 All images are confocal 2 μm thick optical sections. Data are shown as mean ± SEM of the indicated number of the experiments (n) (*$p < 0.05$; **$p < 0.01$; ***$p < 0.001$). Scale bars: in (B) and (C), 10 μm; in (D), 5 μm. See also Figure S6 and Table S1.

generates RS and the activation of a p53- and p21-dependent cell cycle arrest (Marión et al., 2009; Banito and Gil, 2010). Finally, several genomic analyses identified CNV events that were generated de novo during reprogramming, arguing that reprogramming factors can be inducers of RS (Blasco et al., 2011). Hence, stemness is a state that is particularly prone to RS, and stemness factors have been shown to actively induce RS in embryonic cells. We here show that deregulated expression of Sox2 is also a potent inducer of RS in NSCs. Given that oncogenes are known to induce RS (Bartkova et al., 2006; Di Micco et al., 2006), Sox2-induced RS might easily be related to its oncogenic role (Gangemi et al., 2009) and to its high expression in brain tumors (Phi et al., 2008). In agreement with this notion, oncogene-induced RS is exacerbated in the context of a deregulated G1/S checkpoint, such as in the absence of p53 (Toledo et al., 2011). Hence, the findings reported here could be explained by a proproliferative role of Sox2 in NSCs, which generates RS by facilitating promiscuous S-phase entry, and which is limited by p21. Importantly, γH2AX is also seen in vivo in p21-deficient brains, and can be alleviated by the depletion of Sox2 or by an additional copy of the *Chk1* allele. We propose that these observations constitute an in vivo case of RS and senescence induced by a pluripotency factor.

One important difference of our findings from oncogene-induced DNA damage is that the RS observed in NSCs is p21 dependent in a p53-independent manner (Besson et al., 2008). We believe that this could be explained by a limited role of p53 in the regulation of the G1/S transition on NSCs. In support of this view, and in contrast to what is observed in p21-deficient NSCs, lack of p53 in NSCs does not result in their exhaustion (Meletis et al., 2006). Moreover, whereas p53 deficiency is synthetic lethal with the deletion or hypomorphism of ATR at the organism level (Murga et al., 2009; Ruzankina et al., 2009), this synthetic lethal effect is not seen on neural progenitors of the fetal brain (Lee et al., 2012). Hence, p53 seems to play a limited role in suppressing RS on NSCs. It is noteworthy that deletion of p21 in leukemic stem cells has also been shown to exacerbate DNA damage independently of p53, which, similarly to our observation on NSCs, also ends up limiting the self-renewal of these cancer cells (Viale et al., 2009). In this context, p21 would paradoxically be working as an oncogene, since it extends the proliferative lifespan of cancer stem cells by limiting replication-born genomic damage. Whether this role on leukemic stem cells is also related to the abnormal expression of proproliferative stemness factors including Sox2 remains unknown, but in favor of this view, *SOX2* amplifications and altered expression have been found in human cancers that are not only of a brain origin (Bass et al., 2009; Maier et al., 2011). New oncogenic roles for cell cycle inhibitors are now being proposed (Besson et al., 2008) and, for example, PDGF-induced gliomagenesis is reduced in mice lacking p21 (Liu et al., 2007). To what extent p21 might be particularly important in safeguarding the genome of cancer stem cells in SOX2 overexpressing tumors is an interesting venue for future research.

## EXPERIMENTAL PROCEDURES

### Animals

Mice of the *p21* (Brugarolas et al., 1995), *p53* (Donehower et al., 1992), *Chk1* (López-Contreras et al., 2012), and *Sox2* (Avilion et al., 2003) mutant strains were crossed and maintained at the University of Valencia animal core facility in accordance with Spanish regulations (RD1201/2005).

### Cell Culture, Transduction, and Cytometry

Neurospheres were cultured and analyzed as described (Kippin et al., 2005; Ferrón et al., 2007; Andreu-Agulló et al., 2009). Large neurospheres were selected using a 100 μm cell strainer (BD Falcon). Vectors containing *Sox2* shRNAs have been described (Banito et al., 2009). shRNAs for *p53* and *p16/p19$^{Arf}$* were encoded in MLP vectors (Thermofisher). Methods used for retrovirus production, isolation of MEFs, and MEF infection have been described (Banito et al., 2009; Barradas et al., 2009). NSCs were seeded at clonal density and infected overnight by incubation with diluted (1:4) viral supernatants produced in 293T cells (see also Supplemental Information available online). Transduced GFP-positive cells were isolated using a MoFlo cell sorter (Dako). For the reporter assays, 1.6 × 10$^4$ live cells were collected and only the Venus-positive population (about 22%) was analyzed 48 hr postnucleofection in a BD FACSCanto II (BD Biosciences) flow cytometer using FlowJo V7.6.1 (Tree Star Inc.) software.

### Immunocytochemistry

Cells were fixed with 2% paraformaldehyde for 20 min, incubated in blocking buffer (10% normal goat serum and 0.2% Triton X-100 in 0.1M phosphate buffer saline) for 30 min, and incubated overnight at 4°C with the indicated primary antibodies (see Table S1, available online). After several washes with PBS, immunoreactivity was detected with Cy3- or Cy2-conjugated secondary antibodies (1:500; Jackson InmunoResearch Labs.) or with biotinylated antibodies (1:300, Vector Laboratories) followed by Cy2-labeled streptavidin (1:200; Jackson InmunoResearch Labs). Cells were counterstained with 4′,6′,-diamidino-2-phenylindole (DAPI) and mounted with Fluorsave (Calbiochem). For γH2AX, RPA, and 53BP1 stainings, cells were fixed with 1% formaldehyde for 10 min followed by methanol at −20°C for 2 min. Brains were obtained and sectioned as described (Andreu-Agulló et al., 2009). Sections were incubated with the indicated antibodies (Table S1) and immunoreactivity was detected as above. Immunofluorescence quantitative microscopy was done in an InCell Analyzer 1000 using *InCell Investigator* software (GE), and at least 1,000 cells were counted in each acquisition (see Supplemental Experimental Procedures for details). Confocal images were taken in an Olympus Fluoview FV10i scanning confocal microscope and analyzed with the FV10-ASW 2.1 or the public domain Java image processing ImageJ software. For quantitation of Sox2 expression in vivo, immunofluorescent signals in each cell were measured as mean pixel (px) density as follows: above background, 5 px; Sox2$^{high}$ ≥ 50 px; Sox2$^{low}$ = 4–50 px; and Sox2$^{negative}$ ≤ 4 px.

### RNA Isolation and qRT-PCR Analysis

Total RNA was extracted using TRIzol and cDNA synthesized using SuperScript III reverse transcriptase kit (Invitrogen). cDNA products were amplified using an Applied Biosystems StepOne plus Fast Real-Time PCR system. Taqman probes for mouse *Sox2*, *p21*, *p53*, *Gadd45*, *Sigma14-3-3*, and *Gapdh* were purchased from Applied Biosystems. Primer sequences used for qPCR assessment of *p16*, *p19$^{Arf}$*, and control *β2 microglobulin* expression are listed in Table S2.

### ChIP Analysis and Immunoblotting

ChIP procedure on neurospheres has been previously described in detail (Andreu-Agulló et al., 2009). Immunoprecipitated DNA was purified with the Wizard SV Gel and PCR Clean Up System and analyzed by qPCR. Primer pairs gave a single product as confirmed by dissociation curve analysis. The primers used to amplify the UTR and SRR2 regions are listed in Table S2. Immunoblotting was carried out using standard procedures. Antibodies used in these procedures are listed in Table S1.

### Statistical Methods

Results are presented as mean ± SEM of a number (n) of independent experiments. Statistical significance was determined by two-way Student's t tests using SPSS software.

## SUPPLEMENTAL INFORMATION

Supplemental Information for this article includes six Figures, two tables, and Supplemental Experimental Procedures and can be found with this article online at http://dx.doi.org/10.1016/j.stem.2012.12.001.

## ACKNOWLEDGMENTS

We thank R. Lovell-Badge for the Sox2 mouse strain, and K. Nakashima and O. Okuda for mouse Sox2 and SRR2-TK-Venus reporter constructs, respectively. We are grateful to M.J. Palop for help with the mouse colonies and to A. Flores, A. Martínez, and D. Martínez for their assistance with flow cytometry and high content cellular analysis. We thank L. Sevilla and J.M. Morante-Redolat for critical reading of the manuscript and valuable discussions. We also thank members of the I.F. lab for helpful discussions. This work was supported by grants from Spanish Ministerio de Ciencia e Innovación (MICINN) (Programa de Biomedicina, CIBERNED, and RETIC Terapia Celular) and Generalitat Valenciana (Programas Prometeo and ISIC) to I.F.; MICINN and Xunta de Galicia to A.V.; MICINN/Fondo de Investigación Sanitaria to J.T.; MICINN, Association for International Cancer Research (AICR), Howard Hughes Medical Institute, and European Research Council to O.F.-C.; and Medical Research Council, Cancer Research UK, and the Association for International Cancer Research to J.G. J.T. is a Ramón y Cajal investigator and J.G is a EMBO Young Investigator. M.A.M.-T. was funded by a Spanish MICINN/FPI predoctoral fellowship. E.G.-I. is supported by a predoctoral fellowship from Xunta de Galicia. A.J.L. is the recipient of a postdoctoral fellowship from the Spanish Association Against Cancer. A.B. is funded by the Portuguese Fundaçao para Ciência ea Tecnologia. All of the authors designed and discussed the experiments and contributed to the text of the manuscript. M.A.M.-T. conducted most of the experimental work and wrote a draft of the manuscript. A.B. conducted the MEF experiments. E.P. and E.G.-I. carried out the ChIP assays. A.L.-C. generated the *p21-Chk1*$^{Tg}$ mice. J.T. and I.F. conceived the project, supervised the experiments, and wrote the manuscript. The authors declare no competing financial interests.

Received: March 24, 2012
Revised: October 31, 2012
Accepted: November 29, 2012
Published: December 20, 2012

## REFERENCES

Andreu-Agulló, C., Morante-Redolat, J.M., Delgado, A.C., and Fariñas, I. (2009). Vascular niche factor PEDF modulates Notch-dependent stemness in the adult subependymal zone. Nat. Neurosci. *12*, 1514–1523.

Arnold, K., Sarkar, A., Yram, M.A., Polo, J.M., Bronson, R., Sengupta, S., Seandel, M., Geijsen, N., and Hochedlinger, K. (2011). Sox2(+) adult stem and progenitor cells are important for tissue regeneration and survival of mice. Cell Stem Cell *9*, 317–329.

Avilion, A.A., Nicolis, S.K., Pevny, L.H., Perez, L., Vivian, N., and Lovell-Badge, R. (2003). Multipotent cell lineages in early mouse development depend on SOX2 function. Genes Dev. *17*, 126–140.

Bani-Yaghoub, M., Tremblay, R.G., Lei, J.X., Zhang, D., Zurakowski, B., Sandhu, J.K., Smith, B., Ribecco-Lutkiewicz, M., Kennedy, J., Walker, P.R., and Sikorska, M. (2006). Role of Sox2 in the development of the mouse neocortex. Dev. Biol. *295*, 52–66.

Banito, A., and Gil, J. (2010). Induced pluripotent stem cells and senescence: learning the biology to improve the technology. EMBO Rep. *11*, 353–359.

Banito, A., Rashid, S.T., Acosta, J.C., Li, S., Pereira, C.F., Geti, I., Pinho, S., Silva, J.C., Azuara, V., Walsh, M., et al. (2009). Senescence impairs successful reprogramming to pluripotent stem cells. Genes Dev. *23*, 2134–2139.

Barradas, M., Anderton, E., Acosta, J.C., Li, S., Banito, A., Rodriguez-Niedenführ, M., Maertens, G., Banck, M., Zhou, M.M., Walsh, M.J., et al. (2009). Histone demethylase JMJD3 contributes to epigenetic control of INK4a/ARF by oncogenic RAS. Genes Dev. *23*, 1177–1182.

Bartkova, J., Rezaei, N., Liontos, M., Karakaidos, P., Kletsas, D., Issaeva, N., Vassiliou, L.V., Kolettas, E., Niforou, K., Zoumpourlis, V.C., et al. (2006). Oncogene-induced senescence is part of the tumorigenesis barrier imposed by DNA damage checkpoints. Nature *444*, 633–637.

Bass, A.J., Watanabe, H., Mermel, C.H., Yu, S., Perner, S., Verhaak, R.G., Kim, S.Y., Wardwell, L., Tamayo, P., Gat-Viks, I., et al. (2009). SOX2 is an amplified lineage-survival oncogene in lung and esophageal squamous cell carcinomas. Nat. Genet. *41*, 1238–1242.

Besson, A., Dowdy, S.F., and Roberts, J.M. (2008). CDK inhibitors: cell cycle regulators and beyond. Dev. Cell *14*, 159–169.

Blasco, M.A., Serrano, M., and Fernandez-Capetillo, O. (2011). Genomic instability in iPS: time for a break. EMBO J. *30*, 991–993.

Brugarolas, J., Chandrasekaran, C., Gordon, J.I., Beach, D., Jacks, T., and Hannon, G.J. (1995). Radiation-induced cell cycle arrest compromised by p21 deficiency. Nature *377*, 552–557.

Bylund, M., Andersson, E., Novitch, B.G., and Muhr, J. (2003). Vertebrate neurogenesis is counteracted by Sox1-3 activity. Nat. Neurosci. *6*, 1162–1168.

Collado, M., Blasco, M.A., and Serrano, M. (2007). Cellular senescence in cancer and aging. Cell *130*, 223–233.

Devgan, V., Mammucari, C., Millar, S.E., Brisken, C., and Dotto, G.P. (2005). p21WAF1/Cip1 is a negative transcriptional regulator of Wnt4 expression downstream of Notch1 activation. Genes Dev. *19*, 1485–1495.

Di Micco, R., Fumagalli, M., Cicalese, A., Piccinin, S., Gasparini, P., Luise, C., Schurra, C., Garre', M., Nuciforo, P.G., Bensimon, A., et al. (2006). Oncogene-induced senescence is a DNA damage response triggered by DNA hyper-replication. Nature *444*, 638–642.

Donehower, L.A., Harvey, M., Slagle, B.L., McArthur, M.J., Montgomery, C.A., Jr., Butel, J.S., and Bradley, A. (1992). Mice deficient for p53 are developmentally normal but susceptible to spontaneous tumours. Nature *356*, 215–221.

Dotto, G.P. (2000). p21(WAF1/Cip1): more than a break to the cell cycle? Biochim. Biophys. Acta *1471*, M43–M56.

Ellis, P., Fagan, B.M., Magness, S.T., Hutton, S., Taranova, O., Hayashi, S., McMahon, A., Rao, M., and Pevny, L. (2004). SOX2, a persistent marker for multipotential neural stem cells derived from embryonic stem cells, the embryo or the adult. Dev. Neurosci. *26*, 148–165.

Favaro, R., Valotta, M., Ferri, A.L., Latorre, E., Mariani, J., Giachino, C., Lancini, C., Tosetti, V., Ottolenghi, S., Taylor, V., and Nicolis, S.K. (2009). Hippocampal development and neural stem cell maintenance require Sox2-dependent regulation of Shh. Nat. Neurosci. *12*, 1248–1256.

Fernando, R.N., Eleuteri, B., Abdelhady, S., Nussenzweig, A., Andäng, M., and Ernfors, P. (2011). Cell cycle restriction by histone H2AX limits proliferation of adult neural stem cells. Proc. Natl. Acad. Sci. USA *108*, 5837–5842.

Ferri, A.L., Cavallaro, M., Braida, D., Di Cristofano, A., Canta, A., Vezzani, A., Ottolenghi, S., Pandolfi, P.P., Sala, M., DeBiasi, S., and Nicolis, S.K. (2004). Sox2 deficiency causes neurodegeneration and impaired neurogenesis in the adult mouse brain. Development *131*, 3805–3819.

Ferrón, S.R., Andreu-Agullo, C., Mira, H., Sánchez, P., Marqués-Torrejon, M.A., and Fariñas, I. (2007). A combined ex/in vivo assay to detect effects of exogenously added factors in neural stem cells. Nat. Protoc. *2*, 849–859.

Gangemi, R.M., Griffero, F., Marubbi, D., Perera, M., Capra, M.C., Malatesta, P., Ravetti, G.L., Zona, G.L., Daga, A., and Corte, G. (2009). SOX2 silencing in glioblastoma tumor-initiating cells causes stop of proliferation and loss of tumorigenicity. Stem Cells *27*, 40–48.

Graham, V., Khudyakov, J., Ellis, P., and Pevny, L. (2003). SOX2 functions to maintain neural progenitor identity. Neuron *39*, 749–765.

Hong, H., Takahashi, K., Ichisaka, T., Aoi, T., Kanagawa, O., Nakagawa, M., Okita, K., and Yamanaka, S. (2009). Suppression of induced pluripotent stem cell generation by the p53-p21 pathway. Nature *460*, 1132–1135.

Kawamura, T., Suzuki, J., Wang, Y.V., Menendez, S., Morera, L.B., Raya, A., Wahl, G.M., and Izpisúa Belmonte, J.C. (2009). Linking the p53 tumour suppressor pathway to somatic cell reprogramming. Nature *460*, 1140–1144.

Kippin, T.E., Martens, D.J., and van der Kooy, D. (2005). p21 loss compromises the relative quiescence of forebrain stem cell proliferation leading to exhaustion of their proliferation capacity. Genes Dev. *19*, 756–767.

Kopp, J.L., Ormsbee, B.D., Desler, M., and Rizzino, A. (2008). Small increases in the level of Sox2 trigger the differentiation of mouse embryonic stem cells. Stem Cells *26*, 903–911.

Laurent, L.C., Ulitsky, I., Slavin, I., Tran, H., Schork, A., Morey, R., Lynch, C., Harness, J.V., Lee, S., Barrero, M.J., et al. (2011). Dynamic changes in the copy number of pluripotency and cell proliferation genes in human ESCs and iPSCs during reprogramming and time in culture. Cell Stem Cell *8*, 106–118.

Lee, Y., Shull, E.R., Frappart, P.O., Katyal, S., Enriquez-Rios, V., Zhao, J., Russell, H.R., Brown, E.J., and McKinnon, P.J. (2012). ATR maintains select progenitors during nervous system development. EMBO J. *31*, 1177–1189.

Li, H., Collado, M., Villasante, A., Strati, K., Ortega, S., Cañamero, M., Blasco, M.A., and Serrano, M. (2009). The Ink4/Arf locus is a barrier for iPS cell reprogramming. Nature *460*, 1136–1139.

Liu, Y., Yeh, N., Zhu, X.H., Leversha, M., Cordon-Cardo, C., Ghossein, R., Singh, B., Holland, E., and Koff, A. (2007). Somatic cell type specific gene transfer reveals a tumor-promoting function for p21(Waf1/Cip1). EMBO J. *26*, 4683–4693.

López-Contreras, A.J., Gutierrez-Martinez, P., Specks, J., Rodrigo-Perez, S., and Fernández-Capetillo, O. (2012). An extra allele of Chk1 limits oncogene-induced replicative stress and promotes transformation. J. Exp. Med. *209*, 455–461.

Maier, S., Wilbertz, T., Braun, M., Scheble, V., Reischl, M., Mikut, R., Menon, R., Nikolov, P., Petersen, K., Beschorner, C., et al. (2011). SOX2 amplification is a common event in squamous cell carcinomas of different organ sites. Hum. Pathol. *42*, 1078–1088.

Marión, R.M., Strati, K., Li, H., Murga, M., Blanco, R., Ortega, S., Fernandez-Capetillo, O., Serrano, M., and Blasco, M.A. (2009). A p53-mediated DNA damage response limits reprogramming to ensure iPS cell genomic integrity. Nature *460*, 1149–1153.

Meletis, K., Wirta, V., Hede, S.M., Nistér, M., Lundeberg, J., and Frisén, J. (2006). p53 suppresses the self-renewal of adult neural stem cells. Development *133*, 363–369.

Miyagi, S., Saito, T., Mizutani, K., Masuyama, N., Gotoh, Y., Iwama, A., Nakauchi, H., Masui, S., Niwa, H., Nishimoto, M., et al. (2004). The Sox-2 regulatory regions display their activities in two distinct types of multipotent stem cells. Mol. Cell. Biol. *24*, 4207–4220.

Miyagi, S., Nishimoto, M., Saito, T., Ninomiya, M., Sawamoto, K., Okano, H., Muramatsu, M., Oguro, H., Iwama, A., and Okuda, A. (2006). The Sox2 regulatory region 2 functions as a neural stem cell-specific enhancer in the telencephalon. J. Biol. Chem. *281*, 13374–13381.

Miyagi, S., Masui, S., Niwa, H., Saito, T., Shimazaki, T., Okano, H., Nishimoto, M., Muramatsu, M., Iwama, A., and Okuda, A. (2008). Consequence of the loss of Sox2 in the developing brain of the mouse. FEBS Lett. *582*, 2811–2815.

Murga, M., Bunting, S., Montaña, M.F., Soria, R., Mulero, F., Cañamero, M., Lee, Y., McKinnon, P.J., Nussenzweig, A., and Fernandez-Capetillo, O. (2009). A mouse model of ATR-Seckel shows embryonic replicative stress and accelerated aging. Nat. Genet. *41*, 891–898.

Närvä, E., Autio, R., Rahkonen, N., Kong, L., Harrison, N., Kitsberg, D., Borghese, L., Itskovitz-Eldor, J., Rasool, O., Dvorak, P., et al. (2010). High-resolution DNA analysis of human embryonic stem cell lines reveals culture-induced copy number changes and loss of heterozygosity. Nat. Biotechnol. *28*, 371–377.

Nijnik, A., Woodbine, L., Marchetti, C., Dawson, S., Lambe, T., Liu, C., Rodrigues, N.P., Crockford, T.L., Cabuy, E., Vindigni, A., et al. (2007). DNA repair is limiting for haematopoietic stem cells during ageing. Nature *447*, 686–690.

Orford, K.W., and Scadden, D.T. (2008). Deconstructing stem cell self-renewal: genetic insights into cell-cycle regulation. Nat. Rev. Genet. *9*, 115–128.

Phi, J.H., Park, S.H., Kim, S.K., Paek, S.H., Kim, J.H., Lee, Y.J., Cho, B.K., Park, C.K., Lee, D.H., and Wang, K.C. (2008). Sox2 expression in brain tumors: a reflection of the neuroglial differentiation pathway. Am. J. Surg. Pathol. *32*, 103–112.

Pippa, R., Espinosa, L., Gundem, G., García-Escudero, R., Dominguez, A., Orlando, S., Gallastegui, E., Saiz, C., Besson, A., Pujol, M.J., et al. (2012). p27Kip1 represses transcription by direct interaction with p130/E2F4 at the promoters of target genes. Oncogene *31*, 4207–4220.

Rossi, D.J., Bryder, D., Seita, J., Nussenzweig, A., Hoeijmakers, J., and Weissman, I.L. (2007). Deficiencies in DNA damage repair limit the function of haematopoietic stem cells with age. Nature *447*, 725–729.

Ruzankina, Y., Schoppy, D.W., Asare, A., Clark, C.E., Vonderheide, R.H., and Brown, E.J. (2009). Tissue regenerative delays and synthetic lethality in adult mice after combined deletion of Atr and Trp53. Nat. Genet. *41*, 1144–1149.

Shiloh, Y. (2003). ATM and related protein kinases: safeguarding genome integrity. Nat. Rev. Cancer *3*, 155–168.

Sisodiya, S.M., Ragge, N.K., Cavalleri, G.L., Hever, A., Lorenz, B., Schneider, A., Williamson, K.A., Stevens, J.M., Free, S.L., Thompson, P.J., et al. (2006). Role of SOX2 mutations in human hippocampal malformations and epilepsy. Epilepsia *47*, 534–542.

Taylor, W.R., and Stark, G.R. (2001). Regulation of the G2/M transition by p53. Oncogene *20*, 1803–1815.

Toledo, L.I., Murga, M., and Fernandez-Capetillo, O. (2011). Targeting ATR and Chk1 kinases for cancer treatment: a new model for new (and old) drugs. Mol. Oncol. *5*, 368–373.

Viale, A., De Franco, F., Orleth, A., Cambiaghi, V., Giuliani, V., Bossi, D., Ronchini, C., Ronzoni, S., Muradore, I., Monestiroli, S., et al. (2009). Cell-cycle restriction limits DNA damage and maintains self-renewal of leukaemia stem cells. Nature *457*, 51–56.

Wegner, M. (2011). SOX after SOX: SOXession regulates neurogenesis. Genes Dev. *25*, 2423–2428.

Zhao, C., Deng, W., and Gage, F.H. (2008). Mechanisms and functional implications of adult neurogenesis. Cell *132*, 645–660.